

# The radio-lobe shock of Cen A: particle acceleration & environmental impact



Judith Croston

University of  
Hertfordshire

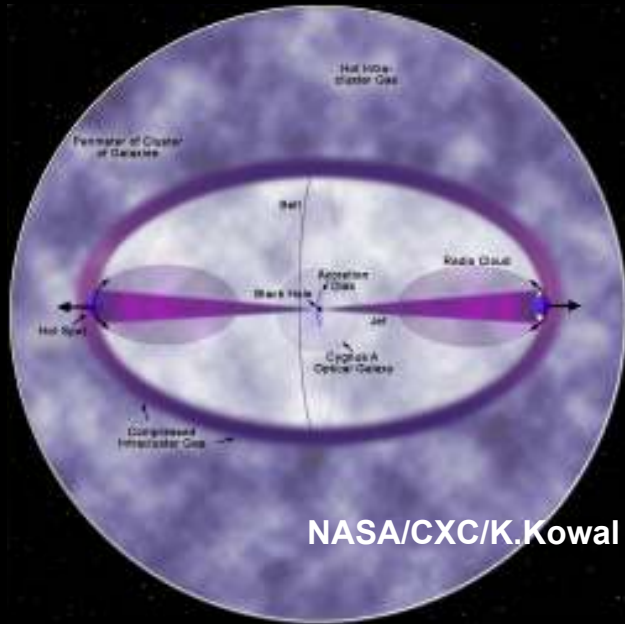


*The Many Faces of Centaurus A*  
*Sydney, Australia 2<sup>nd</sup> July 2009*

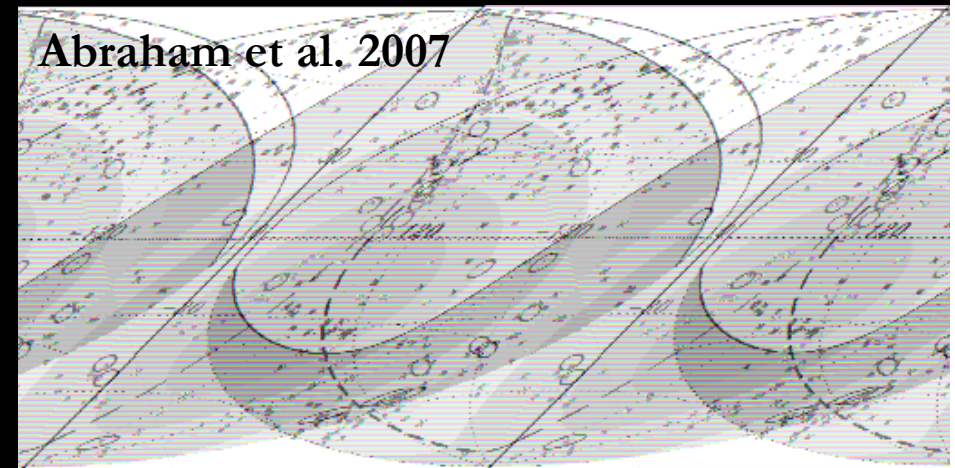
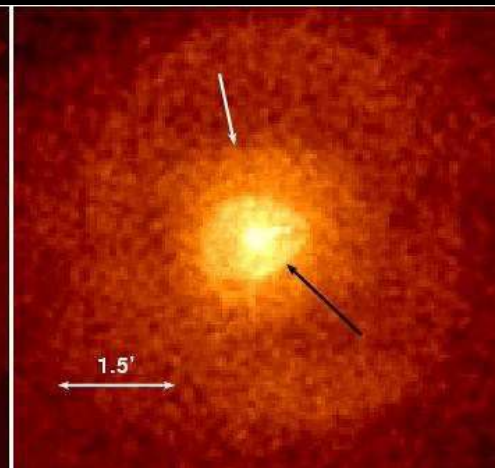
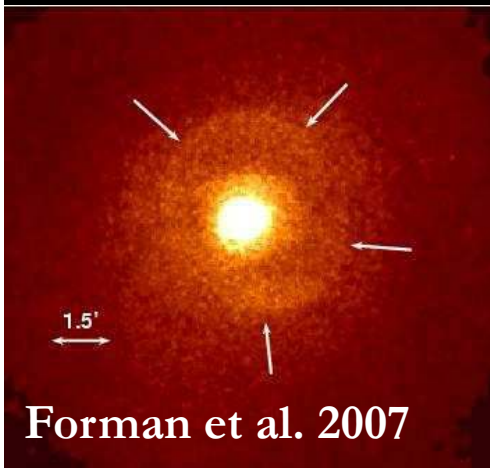
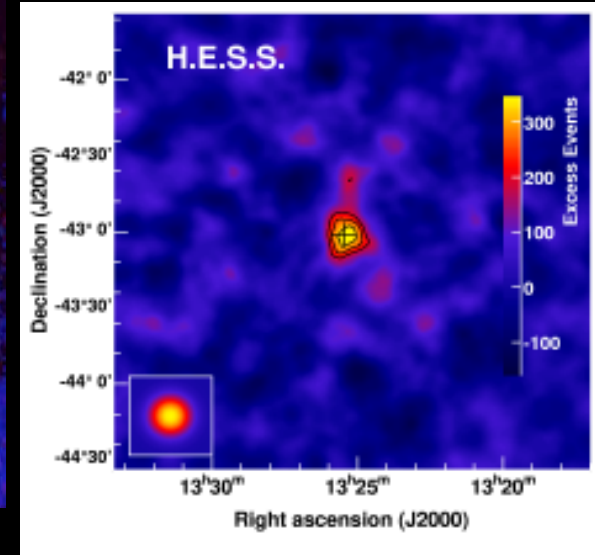
# Outline

- Context: the first detected strong radio-lobe shock
- The non-thermal interpretation of the X-ray feature
- The X-ray structure of the shock region
- Constraints on particle acceleration and magnetic field properties at the shock front
- TeV emission from the shock
- Cosmic rays from the shock
- Implications for shocks and particle acceleration in other radio galaxies

# Some reasons for studying shocks in radio galaxies



Aharonian et al. 2009



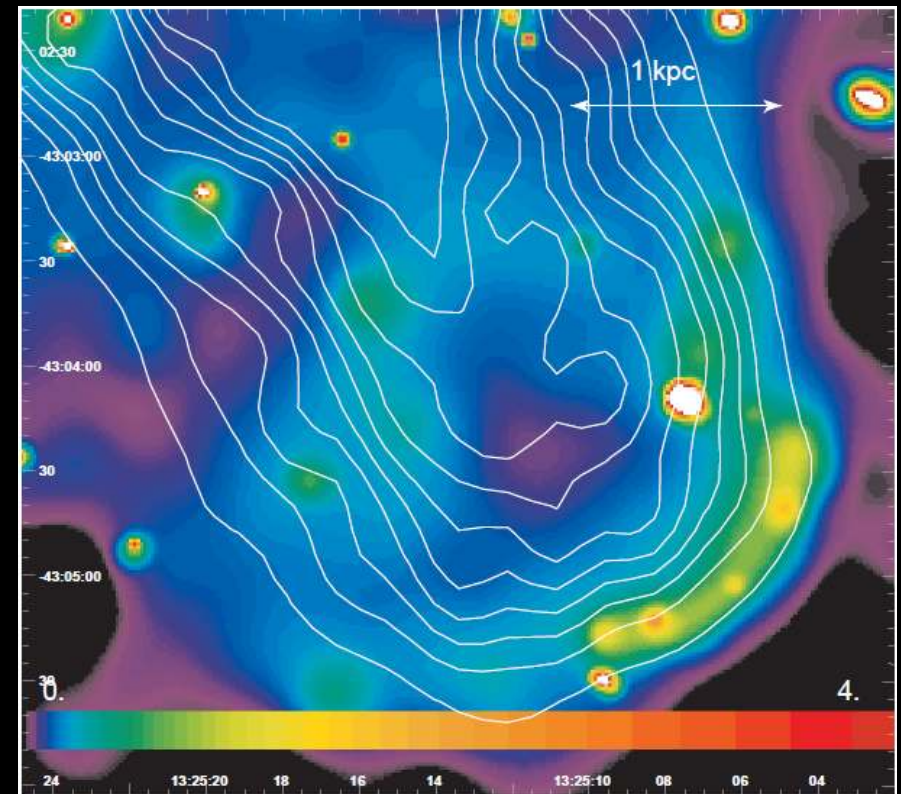
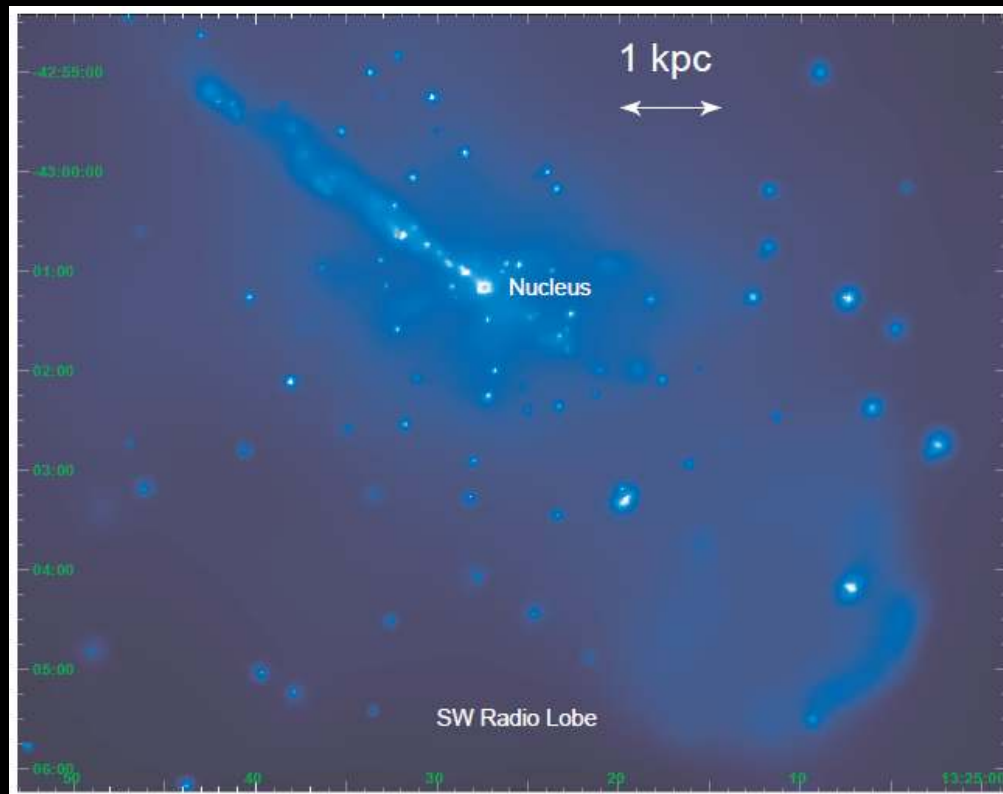
# The radio-lobe shock in Cen A

# Detection of the X-ray shell



- ROSAT detected an X-ray enhancement associated with SW lobe – inferred to be hot gas compressed by lobe expansion.

# Chandra & XMM observations



Kraft et al. 2003

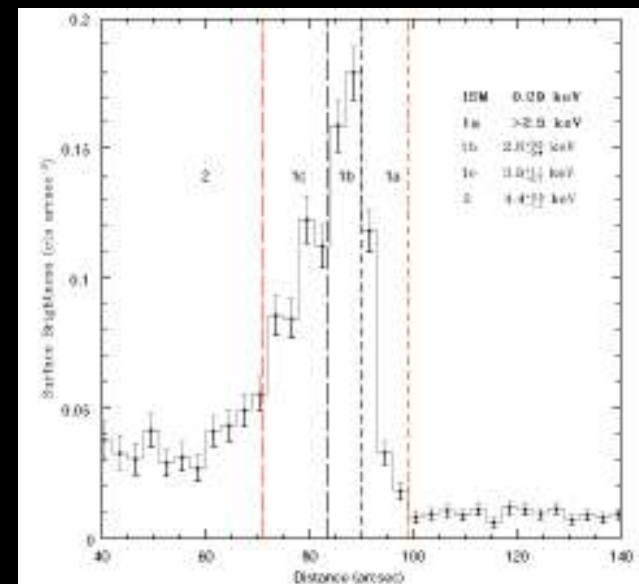
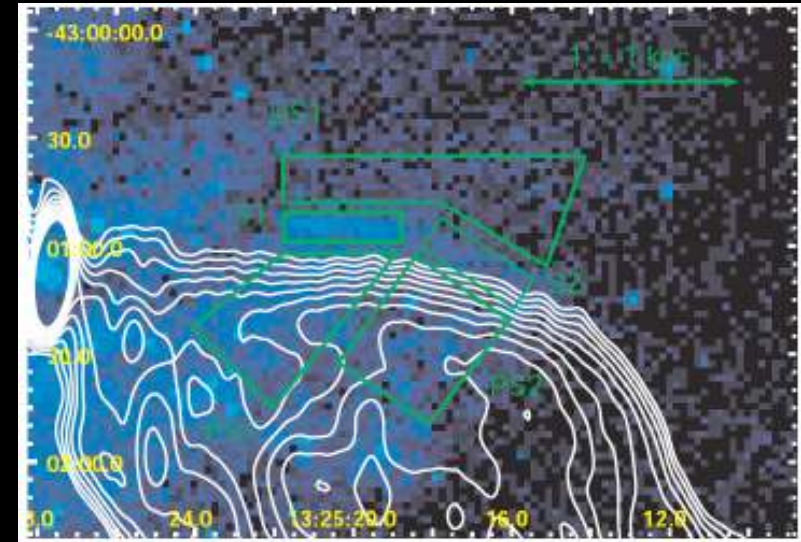
# Initial results

- X-ray shell interpreted as thermal emission from hot gas based on spectrum & lack of non-thermal emission at other wavelengths.
- Pressure-driven expansion of the (inner) radio lobes at Mach  $\sim 8$  is shock heating the ISM of NGC 5128.
- FRIs can be expanding supersonically!
- $\sim 10^{56}$  ergs injected into the ISM
- Direct measure of jet power:  
 $P \sim 10^{42}$  ergs/s

# Temperature structure and transport processes

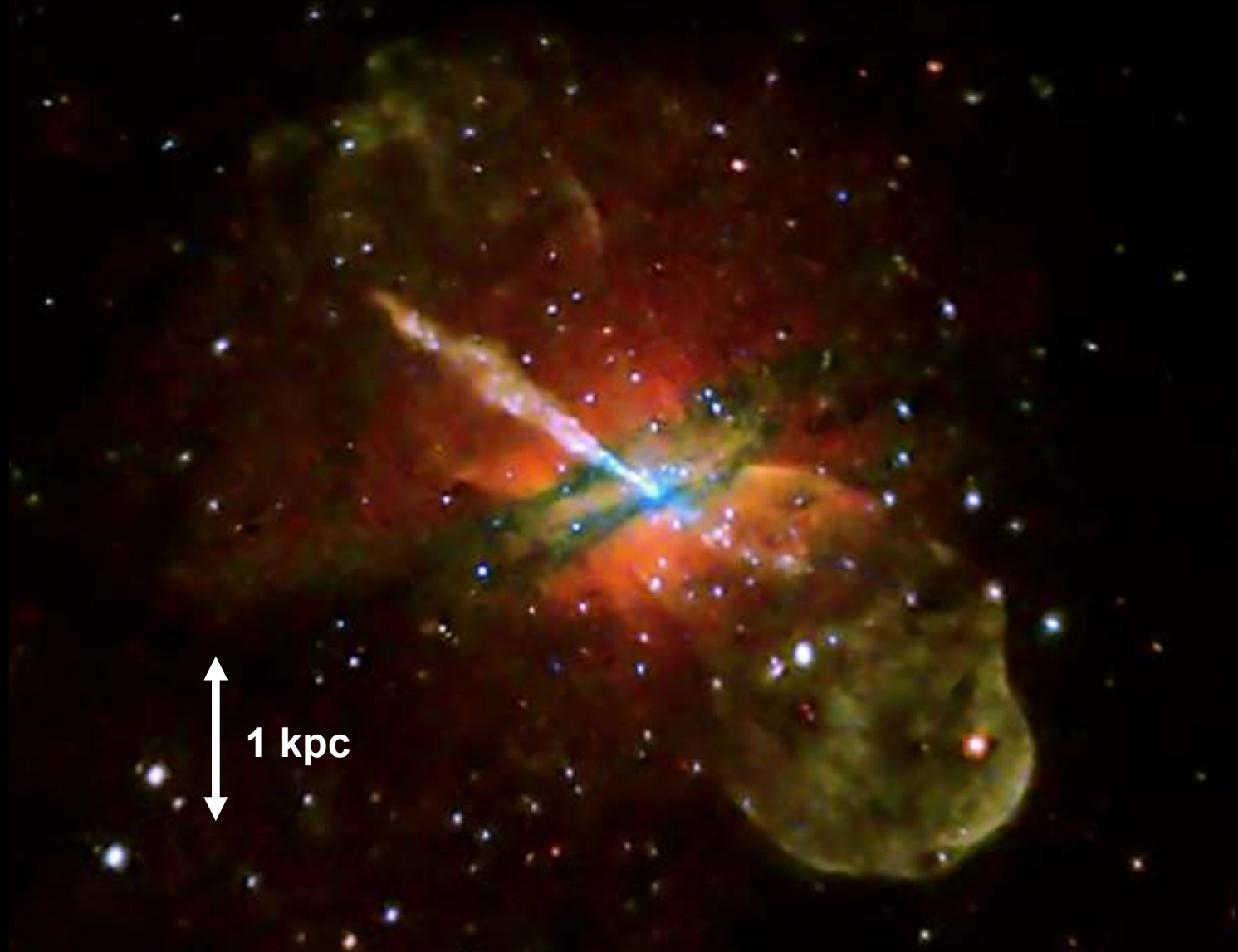
- Shell is cooler closer to the nucleus, as expected for an isobaric lobe expanding into a declining density gradient.
- Tight constraints on size of shocked gas region (between contact discontinuity at radio-lobe edge and shock front) = significantly smaller than scale for electron-ion equilibrium
- => measured  $T_e$  may underestimate shock strength considerably.

Kraft et al. 2007 (~150 ks of Chandra data)



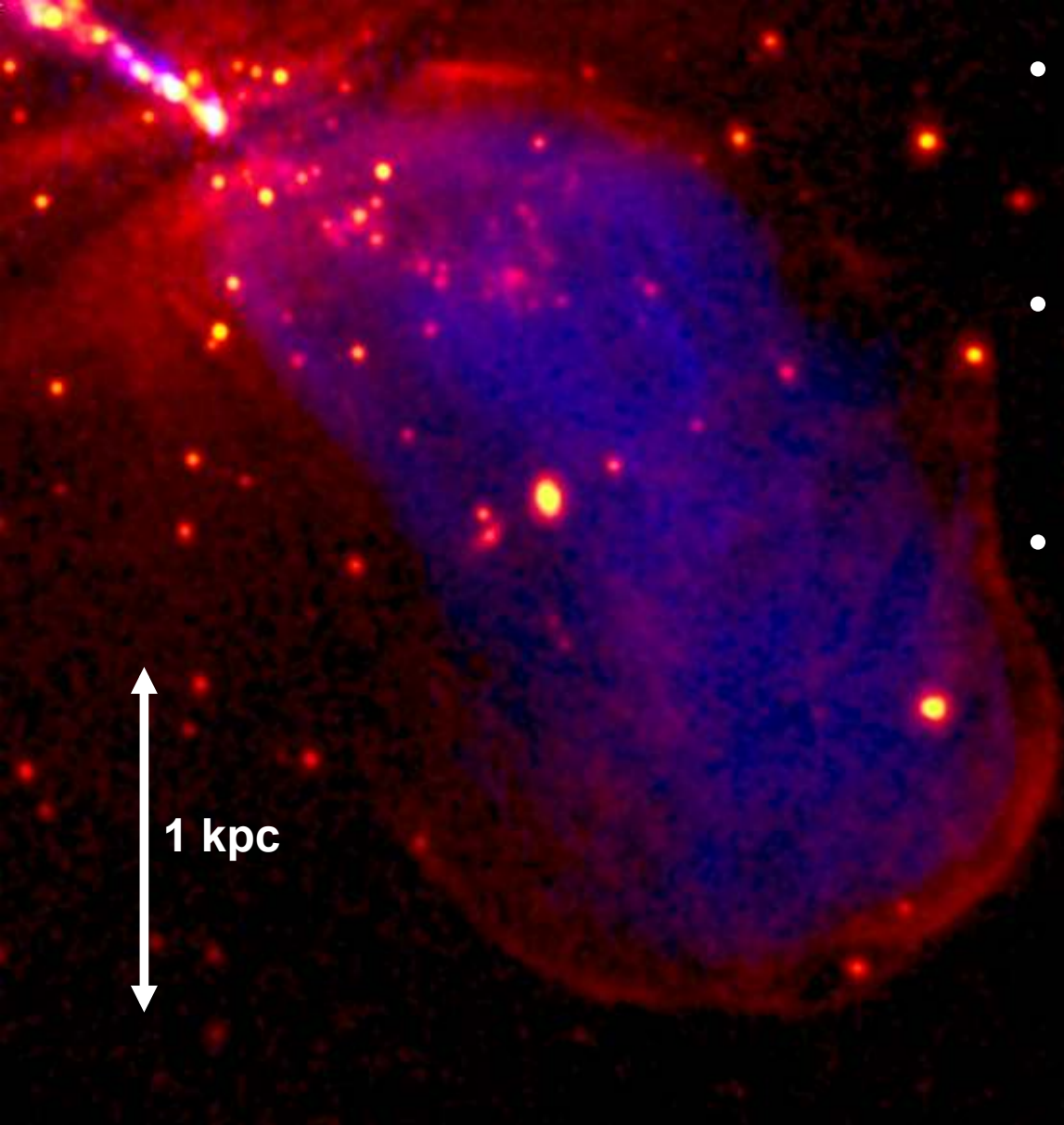
# New results on the X-ray shell

# The Chandra VLP data



# A new interpretation for the X-ray shell

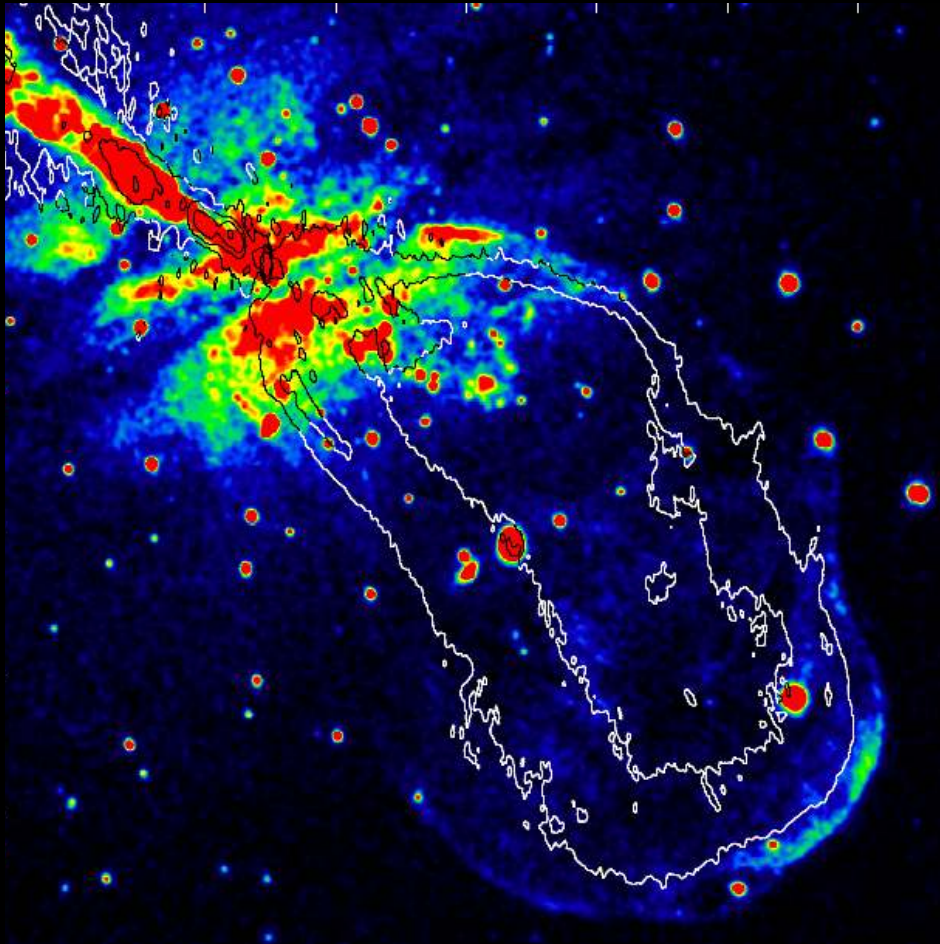
- The new, deeper data reveal most of the X-ray emission is **non-thermal**
- Thermal models for the outer shell can be ruled out at high significance.
- Spectrum well fitted by a power law with  $\Gamma \sim 2.0$ , consistent with an X-ray synchrotron interpretation.

The image shows a large, diffuse X-ray emitting shell, likely from a supernova remnant. The shell is primarily blue and purple, with a bright, multi-colored arc (yellow, orange, red, purple) on the left side. Numerous bright, point-like sources are scattered throughout the field. A white double-headed vertical arrow on the left side indicates a scale of 1 kpc.

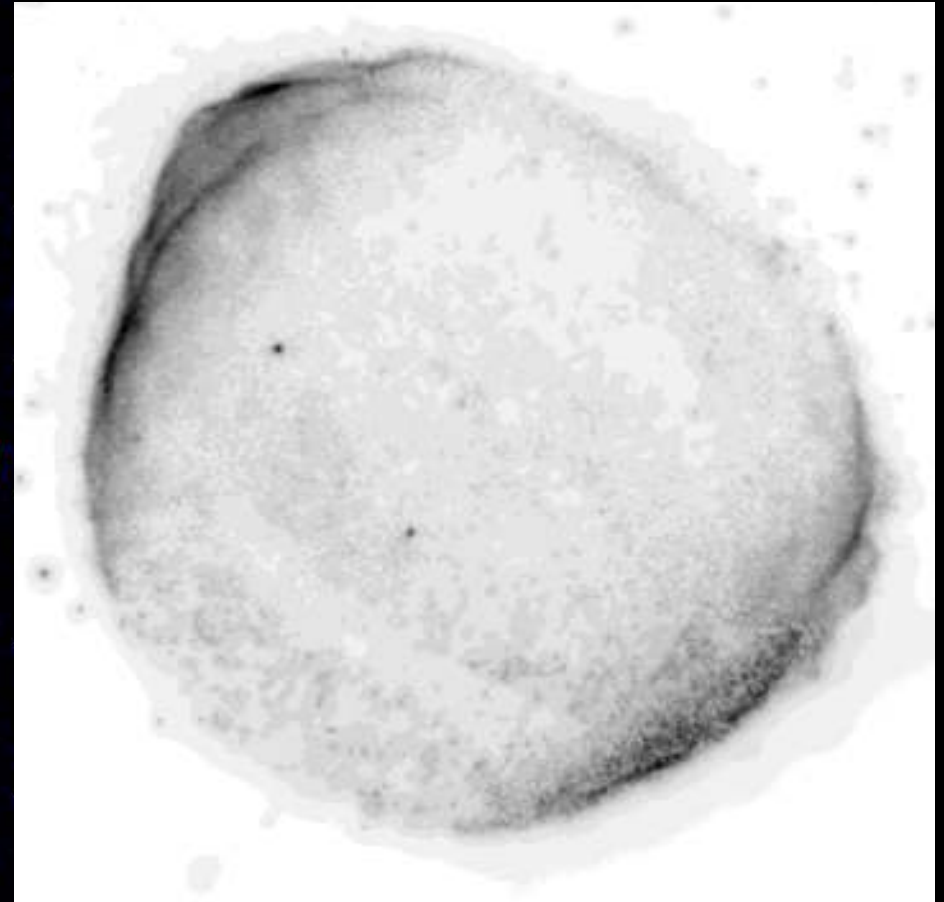
1 kpc

Croston et al. 2009 MNRAS 395 1999

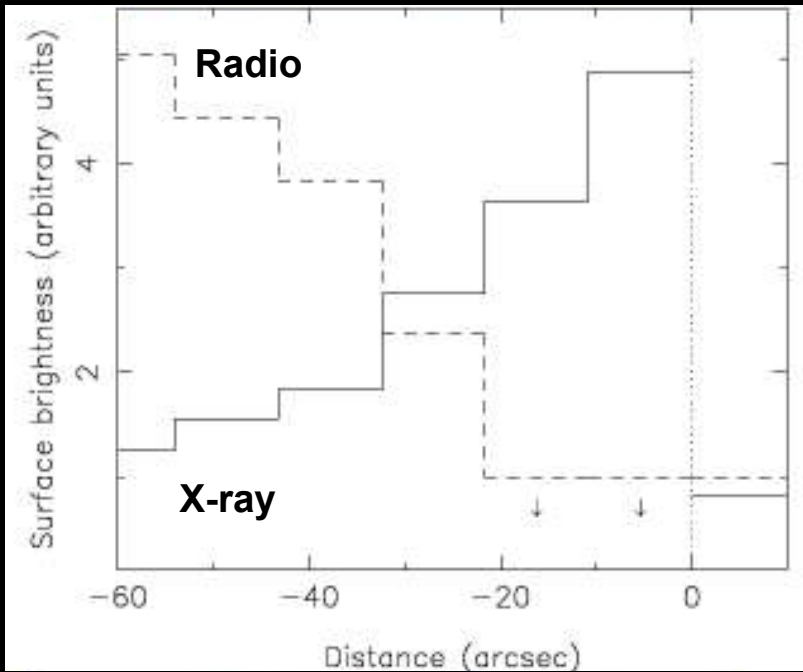
# Particle acceleration at the shock front?



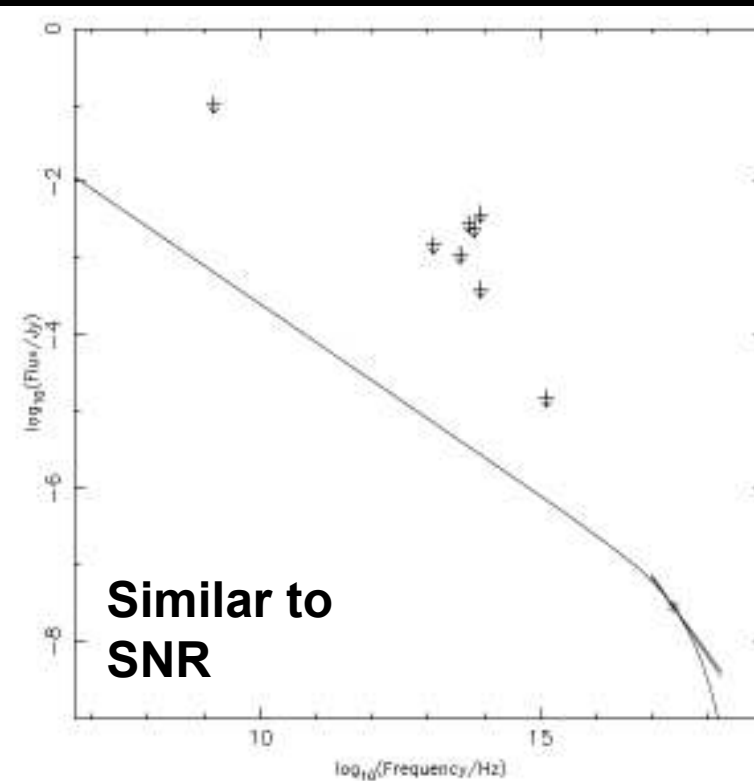
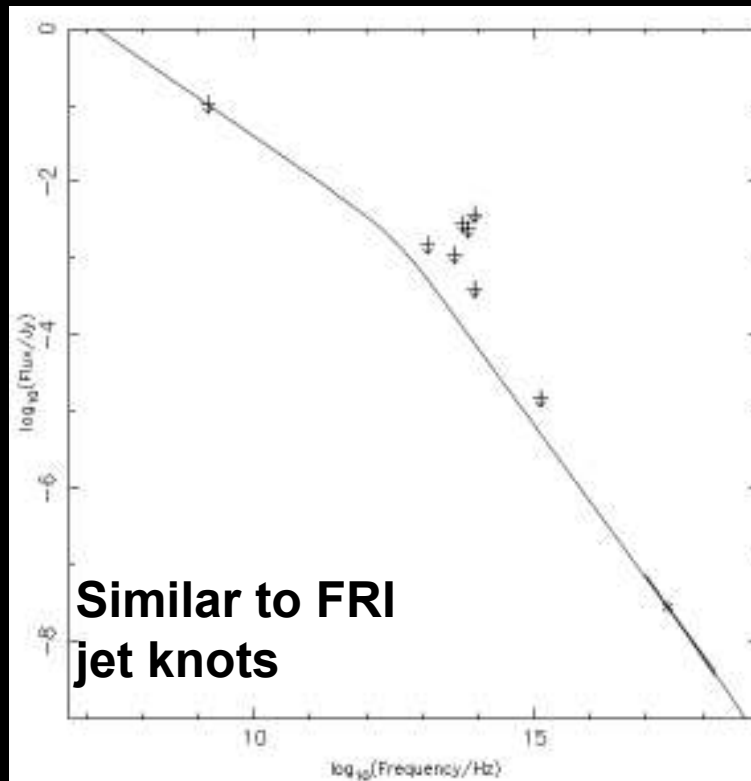
X-ray synchrotron emission  
at the shock front in Cen A



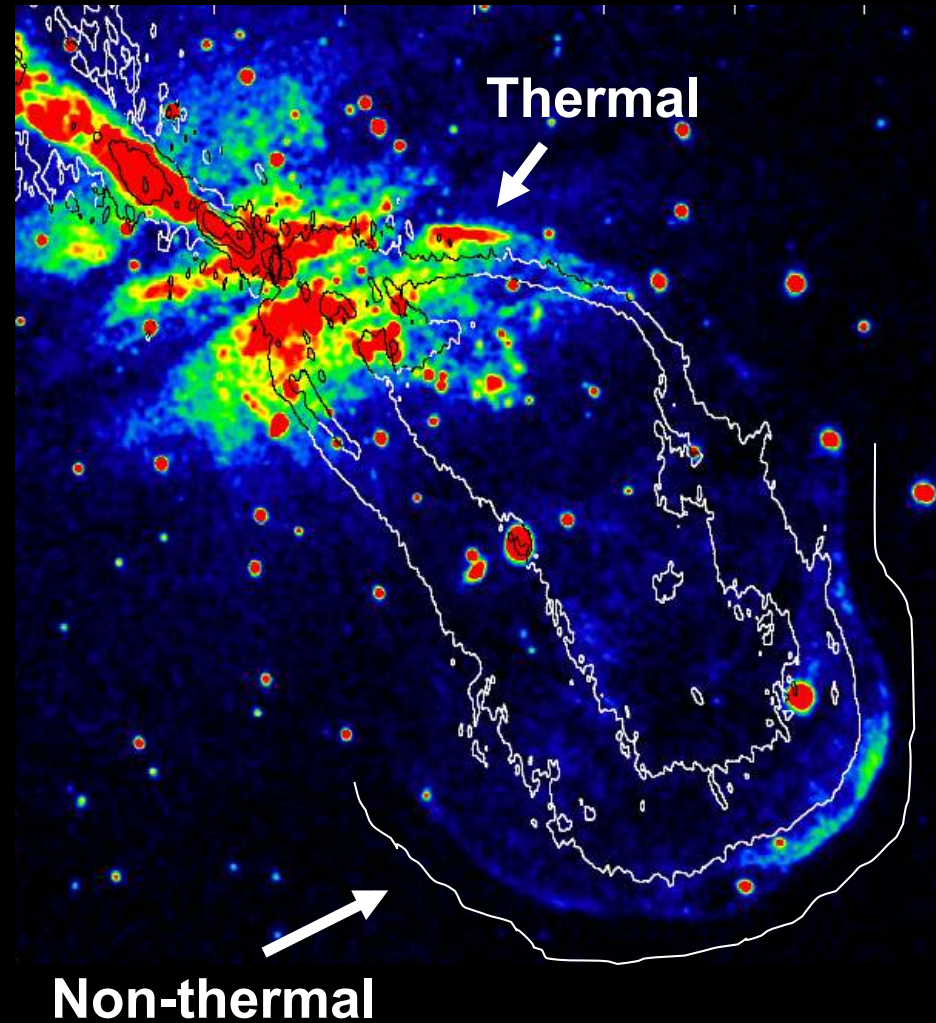
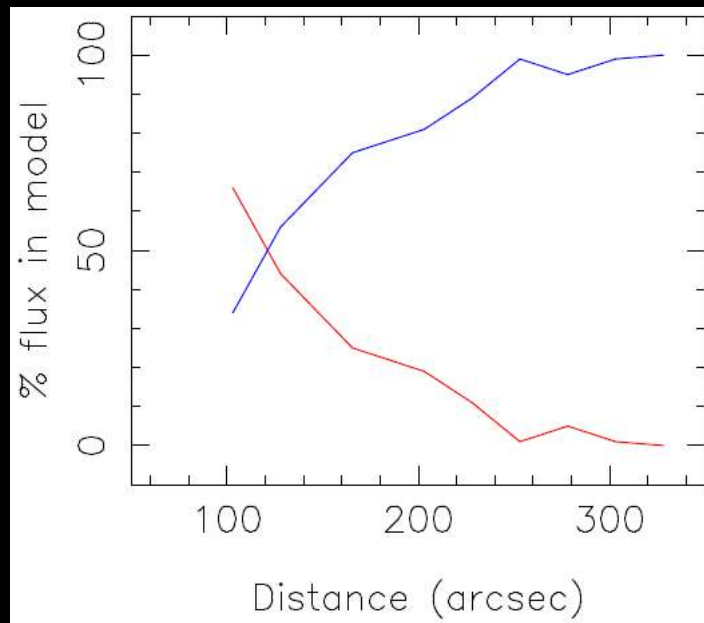
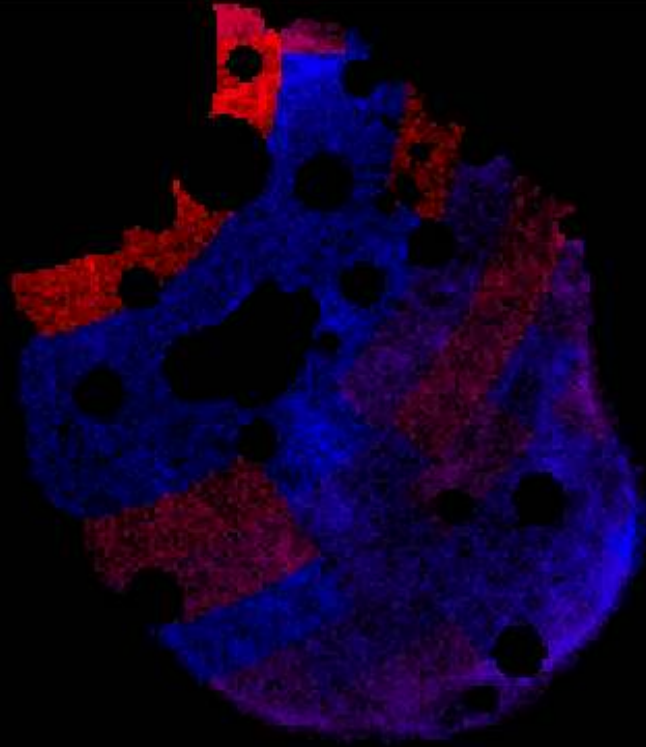
X-ray synchrotron emission  
from SN1006 (Rothenflug et al. 2004)



- The shock front region is not detected in the radio, IR (Spitzer) or UV (GALEX). Deeper Spitzer data coming.
- Limits at these wavelengths don't rule out plausible synchrotron spectra.

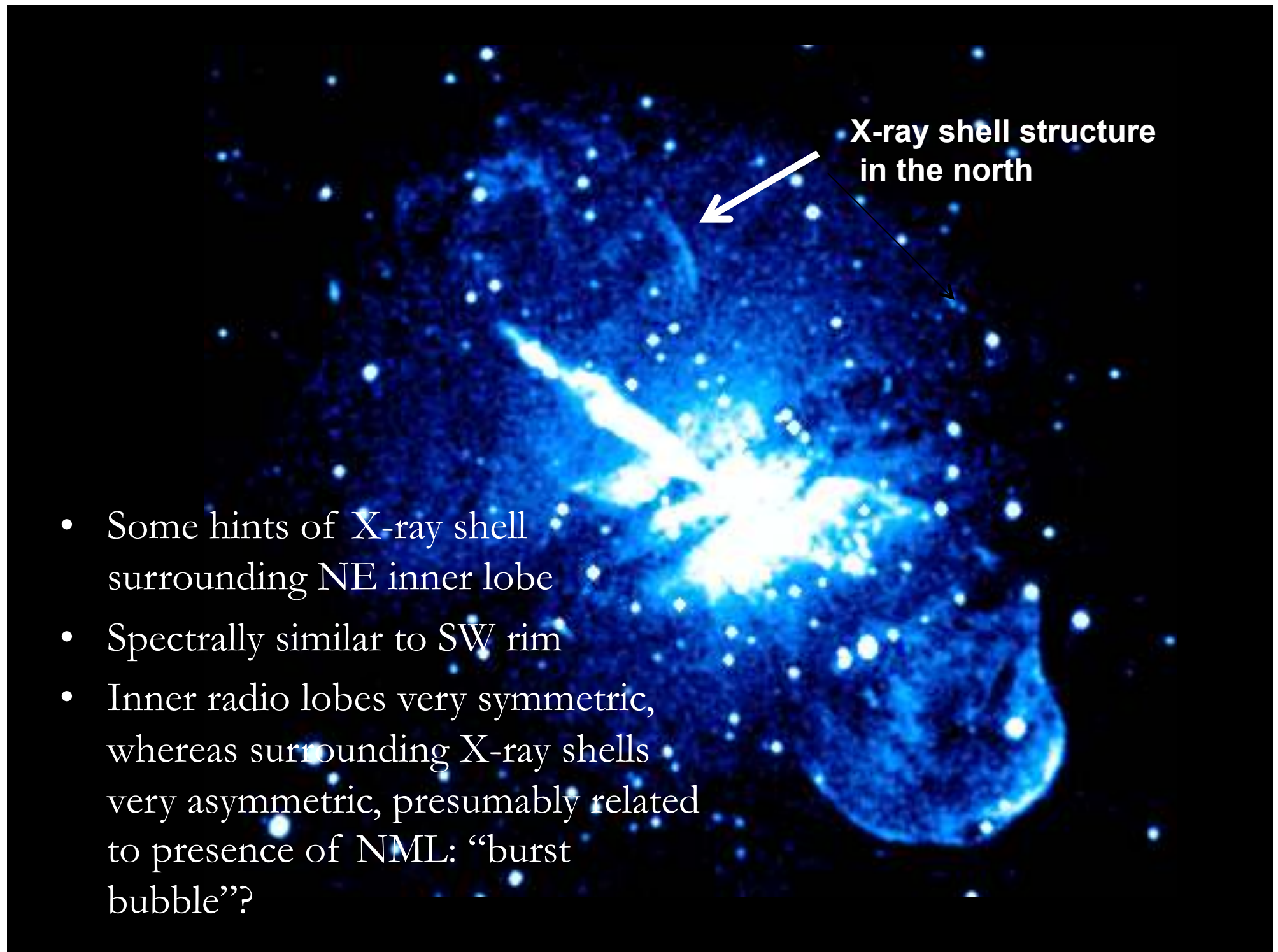


# Spectral structure within the shell



# Shell and lobe dynamics

- Thermal part of the shell (inner region) can be used to investigate shock jump conditions.
- Pressure jump of  $\sim 10x$  implies Mach  $\sim 2.8$  ( $v \sim 850$  km/s) close to the nucleus
- Lobe assumed to be isobaric, so if  $P_{\text{lobe}} = P_{\text{shell}}$ , then can infer pressure jump for outer shell.
- $P_{\text{outer}}/P_{\text{ism}} \sim 87$ , corresponding to Mach  $\sim 8.4$  ( $v = 2600$  km/s)  $\Rightarrow t_{\text{shock}} \sim 10^6$  y
- Inferred expansion speed very similar to SNR with X-ray synchrotron emission (e.g. Vink et al. 2006, Warren et al. 2005, Rothenflug et al. 2004)

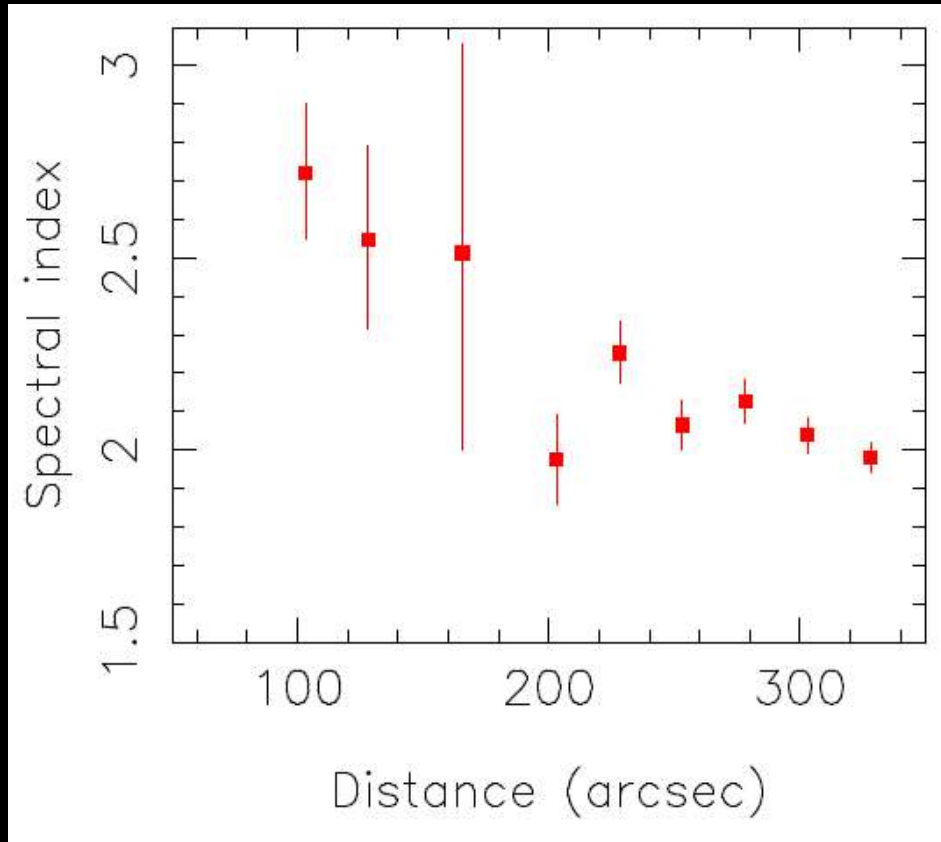


X-ray shell structure  
in the north

- Some hints of X-ray shell surrounding NE inner lobe
- Spectrally similar to SW rim
- Inner radio lobes very symmetric, whereas surrounding X-ray shells very asymmetric, presumably related to presence of NML: “burst bubble”?

Particle acceleration,  
magnetic fields &  
cosmic ray acceleration

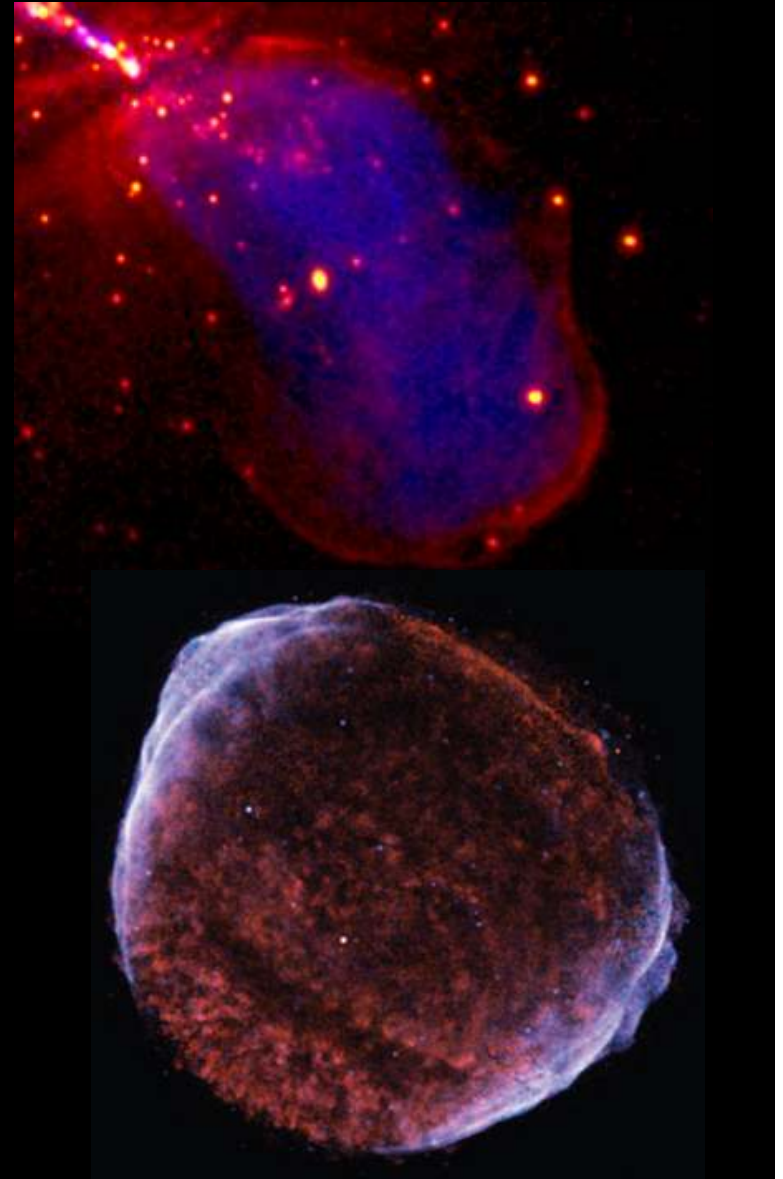
# Particle acceleration constraints



- Flattening of spectral index in outer parts of the shell could be explained by increase in  $\gamma_{\max}$  with shock speed.
- Requires  $\gamma_{\max}$  between  $10^7$  and  $10^9$  over the shock region.
- $\gamma_{\max}$  depends mainly on  $B$  and  $v_{\text{shock}}$  (e.g. Lagage & Cesarsky 1983, Reynolds 1996): for equipartition  $B$ , we find  $\gamma_{\max} \sim 10^8$  at the outer edge, and  $3 \times 10^7$  for the inner ( $v \sim 850$  km/s) region.
- To fit a synchrotron model to the X-ray spectral index at the outer edge, we require  $\gamma_{\max} \sim (2 - 4) \times 10^8$ .

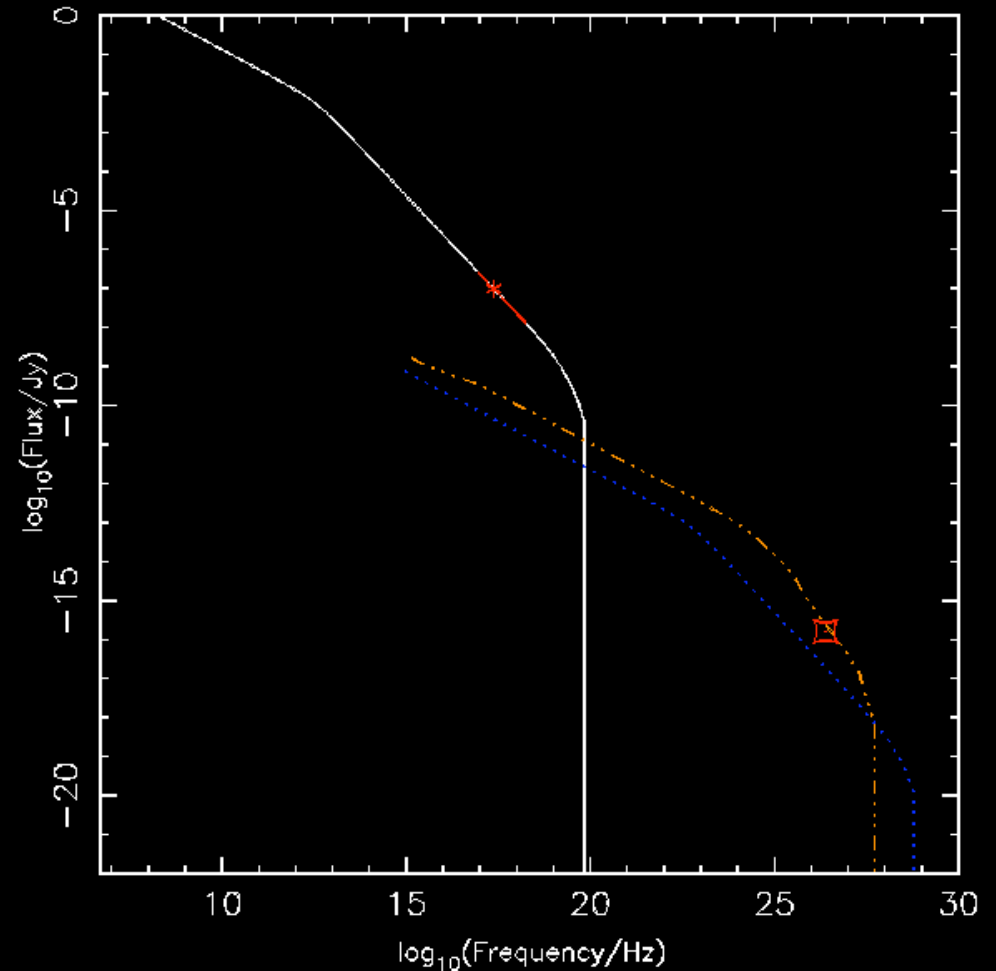
# Particle acceleration & B fields: comparison with SNRs

- SNR shells are inferred to have  $B$  fields  $\gg$  simple compression of the ISM (e.g. Ellison & Vladimirov 2008, Reynolds 2008)  $\Rightarrow$  non-linear DSA with  $B$  amplification (e.g. Bell & Lucek 2001).
- $B$ -field amplification by factors of 10 – 100 plausible in Cen A ( $B_{\text{eq}} \sim 8 \mu\text{G}$  for  $\kappa=1$  and  $\sim 30 \mu\text{G}$  for  $\kappa=100$ ).
- Spectral indices somewhat steeper in SNRs (typically  $\Gamma \sim 2.5$ ), consistent with lower  $E_{\text{max}}$ .



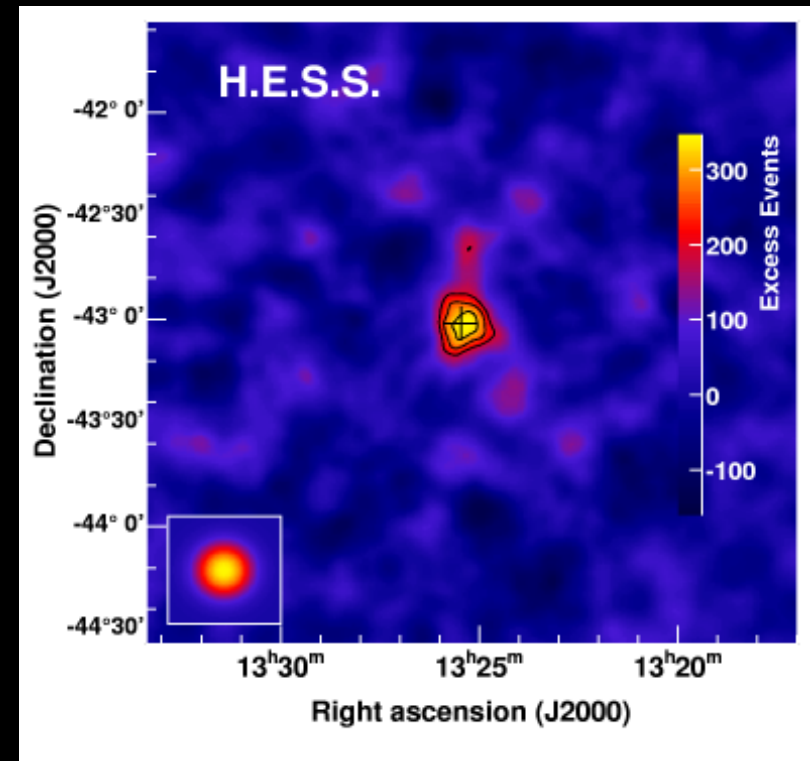
# TeV emission from the shell?

- X-ray synchrotron from the shell implies electrons with TeV energies, hence IC emission in the TeV range might be expected.
- Scattering of galaxy starlight and CMB should result in TeV emission from the shell at detectable levels.
- Recent HESS detection (Aharonian et al. 2009) consistent with our prediction for  $B \sim 7 \mu\text{G}$  ( $\Gamma$  also in agreement), but more probable it's associated with inner regions.



# Implications of HESS detection

- If the inner-lobe shock only responsible for small fraction of the HESS flux, then tight limits on  $B$  in shell.
- Implies  $B \gg 7 \mu\text{G}$ , consistent with equipartition fields if  $\kappa \sim 100$ .
- Consistent with shock behaviour similar to SNR including  $B$  amplification.
- Important implications for Cen A as a source of UHECRs...



Aharonian et al. 2009

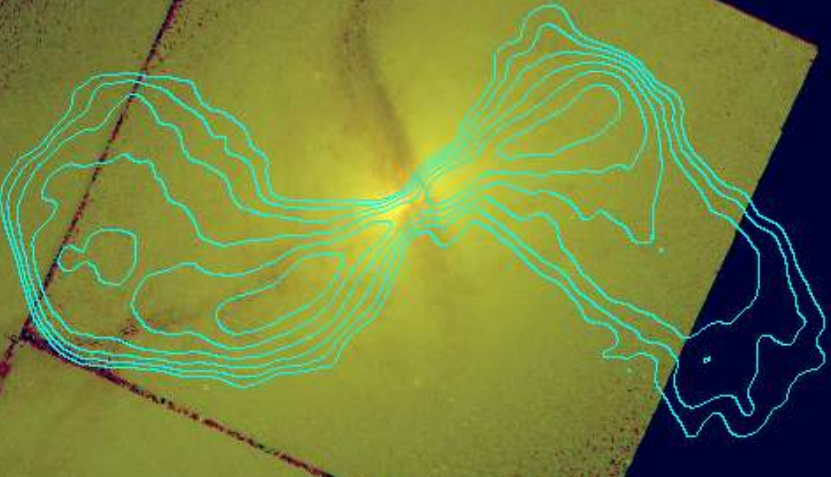
# Cosmic rays from the radio-lobe shock?

- Recent results from the Pierre Auger observatory point to nearby AGN, and Cen A in particular, as a source of the highest energy cosmic rays (Abraham et al. 2007, Moskalenko et al. 2008)
- For an acceleration region of  $\sim 300$  pc, and  $B \sim 8.5 \mu\text{G}$ , typical particle energies won't exceed  $\sim 2 \times 10^{18}$  eV
- Postshock  $B$  would need to be much higher than equipartition value for the shell to accelerate UHECRs ( $\sim 350 \mu\text{G}$  or higher) .
- HESS detection would be consistent with such high  $B$  fields.
- If we are indeed observing  $\gamma_{\text{max}}$  in the X-ray region, then maximum electron energy is  $\sim 10^{14}$  eV; however, if  $\gamma_{\text{max}}$  is dominated by losses it could be significantly higher for protons.

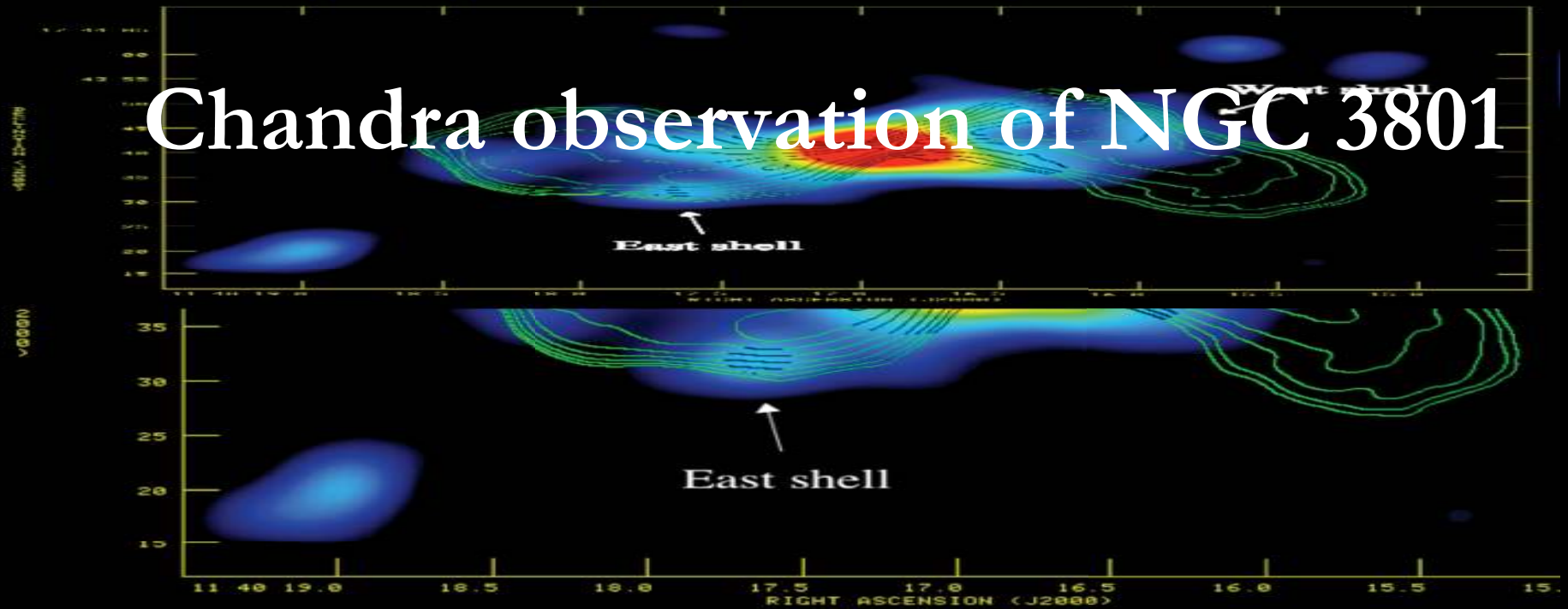
# Radio-lobe shocks in other galaxies

# NGC 3801

HST F814W (red) &  
F555W (green):  
VLA 1.5-GHz  
contours

- $z = 0.0113$
  - disturbed, isolated elliptical
  - Radio source with very similar morphology to Cen A inner lobes, but no evidence for larger-scale radio structure
  - 60-ks *Chandra* observation to look for shocks similar to Cen A
- 

# Chandra observation of NGC 3801



Croston et al. 2007 ApJ, 660, 191

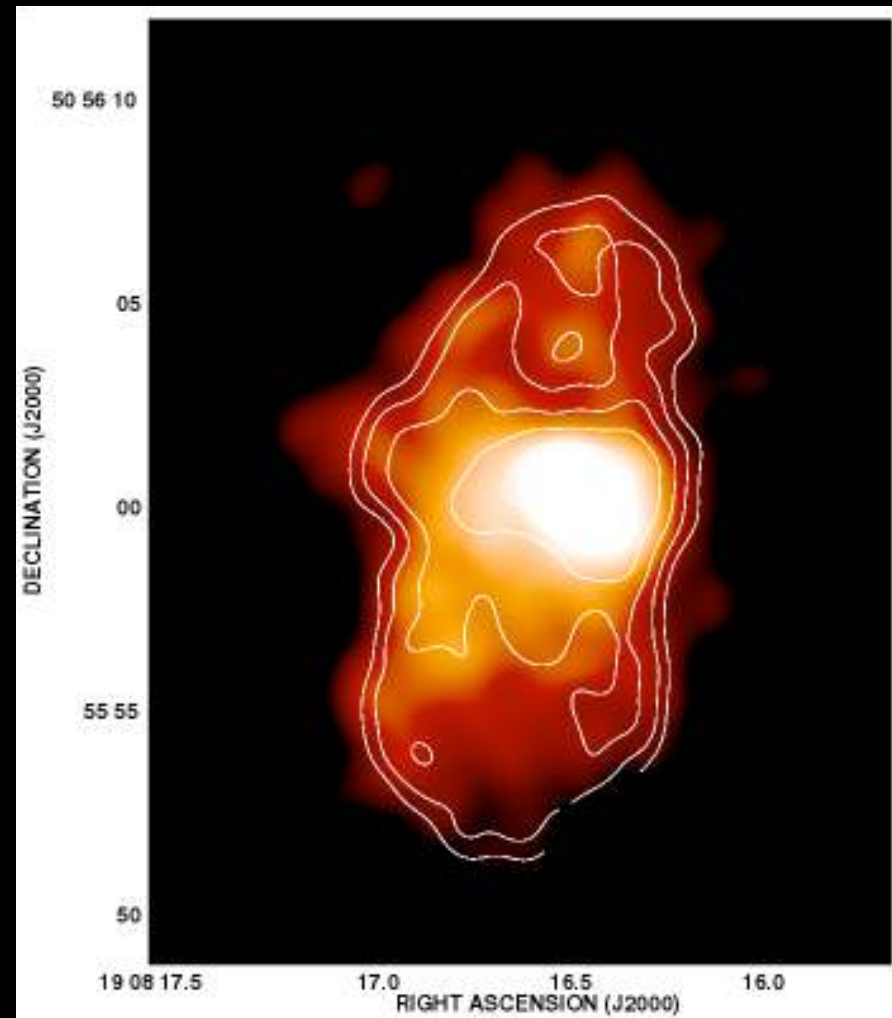
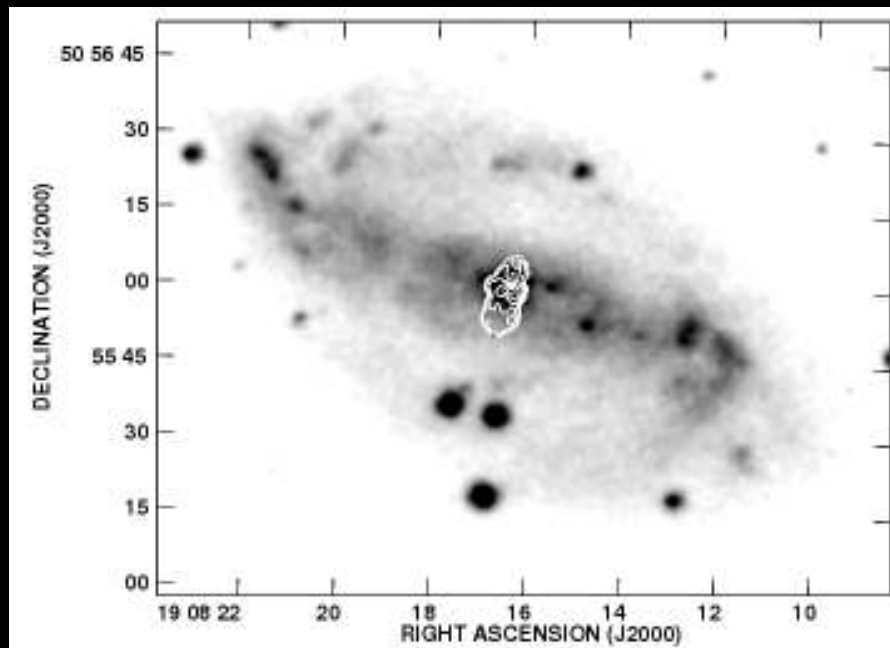
# Physical properties of the X-ray shells in NGC 3801

- *Non-thermal model ruled out* (strong Fe L complex).
- Shells have  $kT = 1.0$  keV (W) &  $0.7$  keV (E); ISM has  $kT = 0.23$  keV
- Density jump consistent with 4, as expected for strong shock.
- Using observed temperature jump, Rankine-Hugoniot conditions give  $\mathcal{M} = 3.8 \pm 1.3$  (W) and  $3.2 \pm 1.0$  (E)
- Implies an expansion speed of  $600\text{-}1200$  km s<sup>-1</sup> => comparable to inner region of Cen A where no particle acceleration observed.
- Total energy in shells,  $1.7 \times 10^{56}$  ergs, is equivalent to thermal energy of ISM within 11 kpc (or 25% of thermal energy within 30 kpc) – similar to Cen A energetics.
- A couple of other examples with less good X-ray data: e.g. NGC 1052, B2 0838+32A (Jetha et al. 2008 MNRAS 391 1052)

# AGN shock-heating in spirals

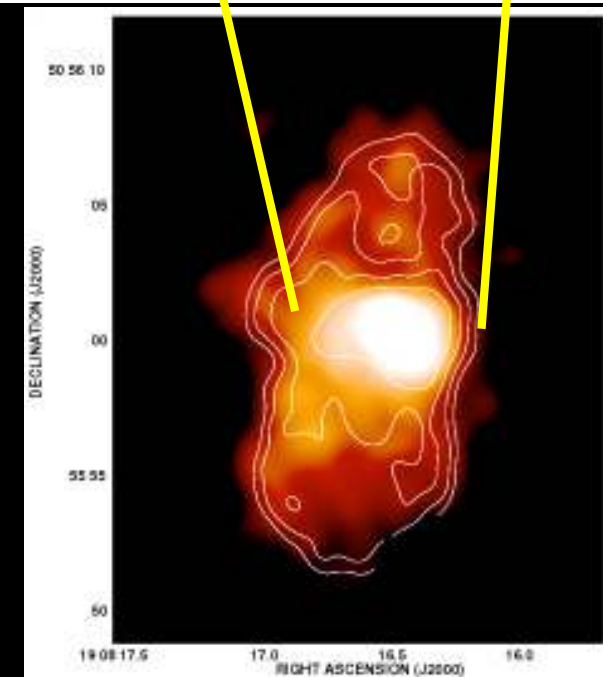
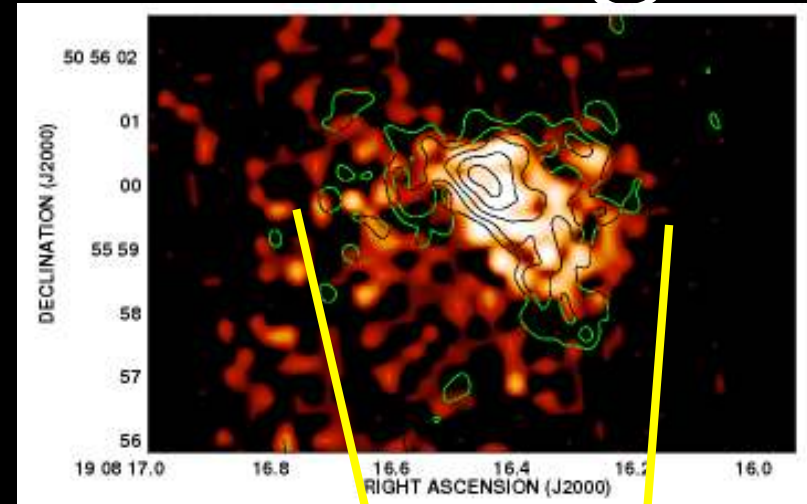
- NGC 6764 is a Seyfert with kpc-scale radio synchrotron bubbles (one of  $\sim 25$  known examples – e.g. Hota & Saikia 2006; Gallimore et al. 2006)
- New Chandra data reveal bubbles of  $\sim 0.8$  keV gas closely matching the radio structure.

Croston et al. 2008 ApJ 688 190



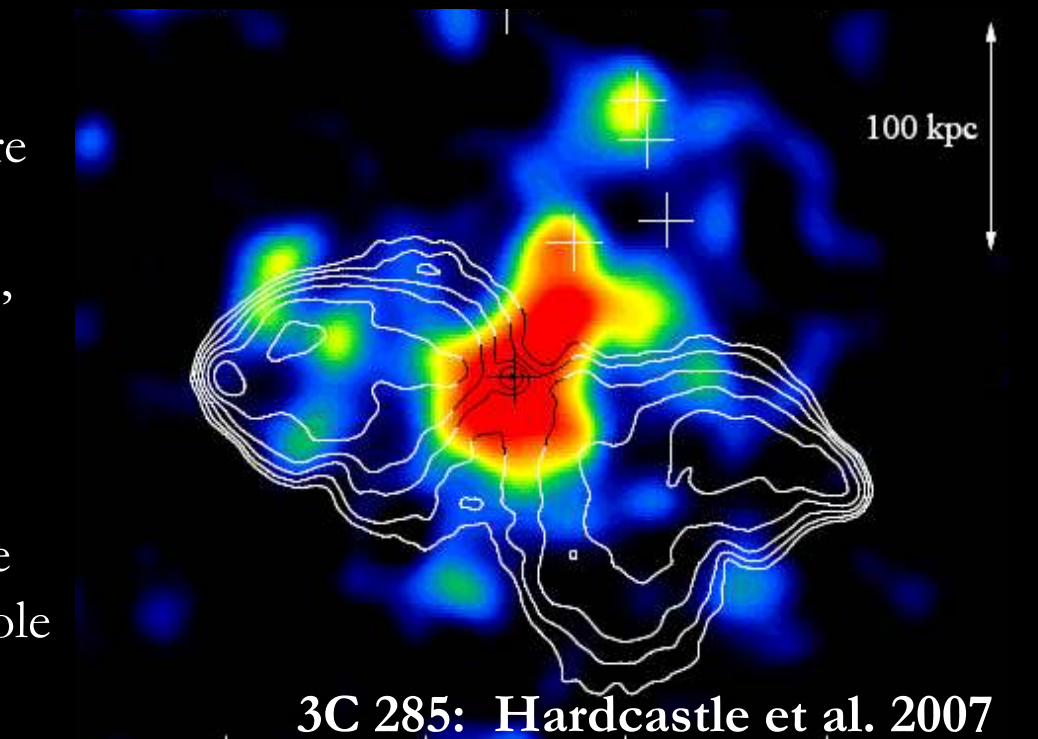
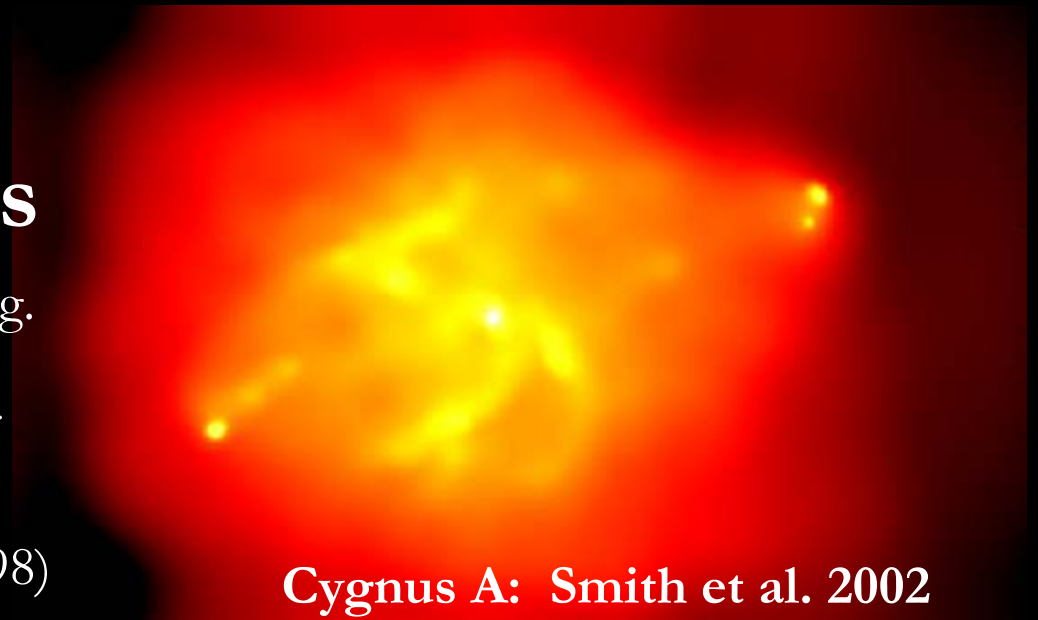
# AGN or starburst heating?

- X-ray bubbles are 2x more luminous than any known starburst wind, while estimated SFR is at least 3x lower.
- Sharp drop in X-ray surface brightness at bubble edges – inconsistent with freely expanding wind.
- E-W radio outflow from AGN associated with brighter X-ray emission from hotter gas.
- Model where disrupted inner jet entrains and shock-heats ISM gas into the kpc-scale bubbles is favoured.
- Some similar Seyferts: NGC 1068 (Young et al. 2001), M51 (Terashima & Wilson 2001), Circinus?
- Energy in bubbles similar to that in NGC 3801 and Cen A ( $\sim 10^{55}$  erg)



# Shocks & particle acceleration in FRIIs

- Self-similar models of FRII lobes (e.g. Kaiser & Alexander 1997) assume strong over-pressuring (Model A of Scheuer et al. 1974) => predict shocked cocoon (e.g. Heinz et al 1998)
- So far only weak shocks found (e.g. Cygnus A: Smith et al. 2002)
- Unlike Cyg A, many nearby FRIIs are in gas-poor environments (e.g. Croston et al. 2004, Kraft et al. 2005, 2007) so may be more highly supersonic.
- Evidence that some FRII lobes are close to pressure balance (Hardcastle et al. 2002, Croston et al. 2004, Belsole et al. 2004, 2007)



# Should we see X-ray synchrotron shells around FR II lobes?

- If FR IIs have similar shock conditions to Cen A, we might expect to detect X-ray synchrotron shells around them.
- Using nearby FR II 3C 33 as an example, it is plausible for its lobes to expand at similar speed to Cen A, so we assume similar particle acceleration efficiency and

$$n_{\text{CR}} \propto n_{\text{shocked}} \propto n_{\text{ISM}}$$

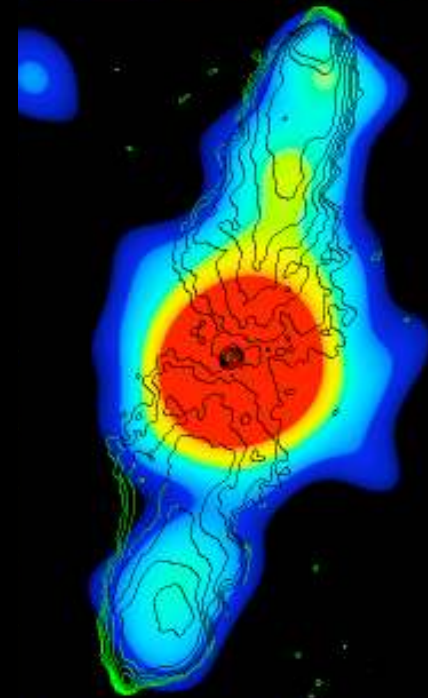
- Expected X-ray synchrotron flux should scale as:

$$S \propto n_{\text{ism}} V D_L^{-2}$$

- $V_{3\text{C}33}/V_{\text{CenA}} \sim 7500$ ;  $n_{3\text{C}33}/n_{\text{CenA}} \sim 0.01$ ;  $D_{3\text{C}33}/D_{\text{CenA}} \sim 72$ ,  
 $\Rightarrow$  predicts a shell flux a factor  $\sim 70$  lower than Cen A,  
 $\sim 1 \text{ nJy}$

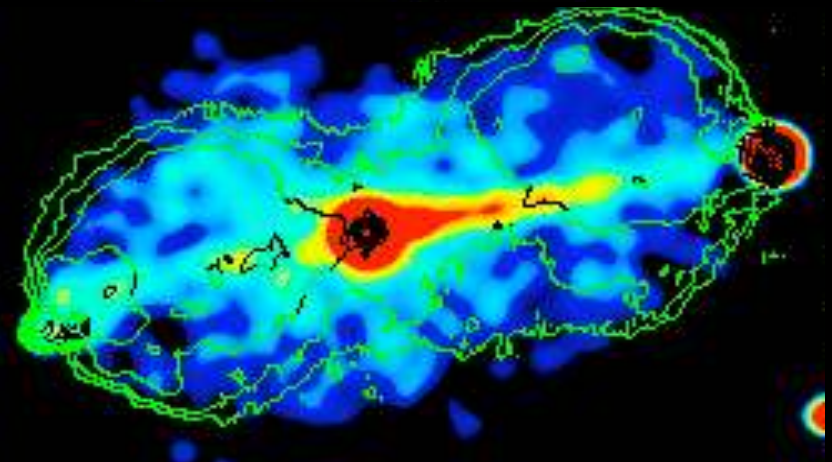
# Should we see X-ray synchrotron shells around FR II lobes?

- Expected flux levels are a significant fraction of those from lobe IC/CMB (e.g. Croston et al. 2005 ApJ 626 733).
- No evidence for edge-brightening in FRIIs & spectral indices flatter than Cen A ( $\Gamma = 1.5 - 1.7$ ) so lobe IC/CMB must dominate
- 3C 33 is relatively nearby – predicted X-ray synchrotron flux drops as distance squared, whereas lobe IC/CMB predictions don't, so will be difficult to constrain this process except in the nearest FRIIs.



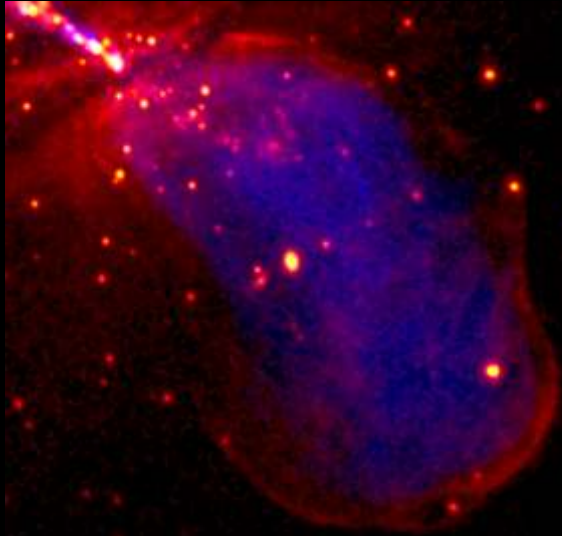
Croston et al. 2004

Hardcastle & Croston 2005



# Summary

- The inner radio-lobe shock in Cen A is accelerating particles to X-ray emitting energies, with shock properties similar to SNR such as SN1006.
- Significant magnetic field amplification may be occurring.
- $B$  appears too low for the shock to accelerate UHECRs: the outer lobes may be a more plausible origin for the PAO events.
- TeV emission from IC scattering by the shell electrons is predicted; level is consistent with recent HESS detection – if only a fraction of the HESS flux comes from the shell this places tight constraints on  $B$ .
- Radio-galaxy shocks, now seen in a few other galaxies (including spirals!) can inject the energy of  $\sim 1$  million SNe, and will have a long-term impact on the host galaxy ISM – given their short lifetimes, such episodes could be common in massive galaxies.
- Particle acceleration at radio-lobe shocks could occur in powerful FRIIs, but X-ray synchrotron shells difficult to detect beyond modest redshifts.
- Details of Cen A shock results in Croston et al. 2009 MNRAS 395 1999



# Thanks to:

Ralph Kraft

Martin Hardcastle

Paul Nulsen

Mark Birkinshaw

Diana Worrall

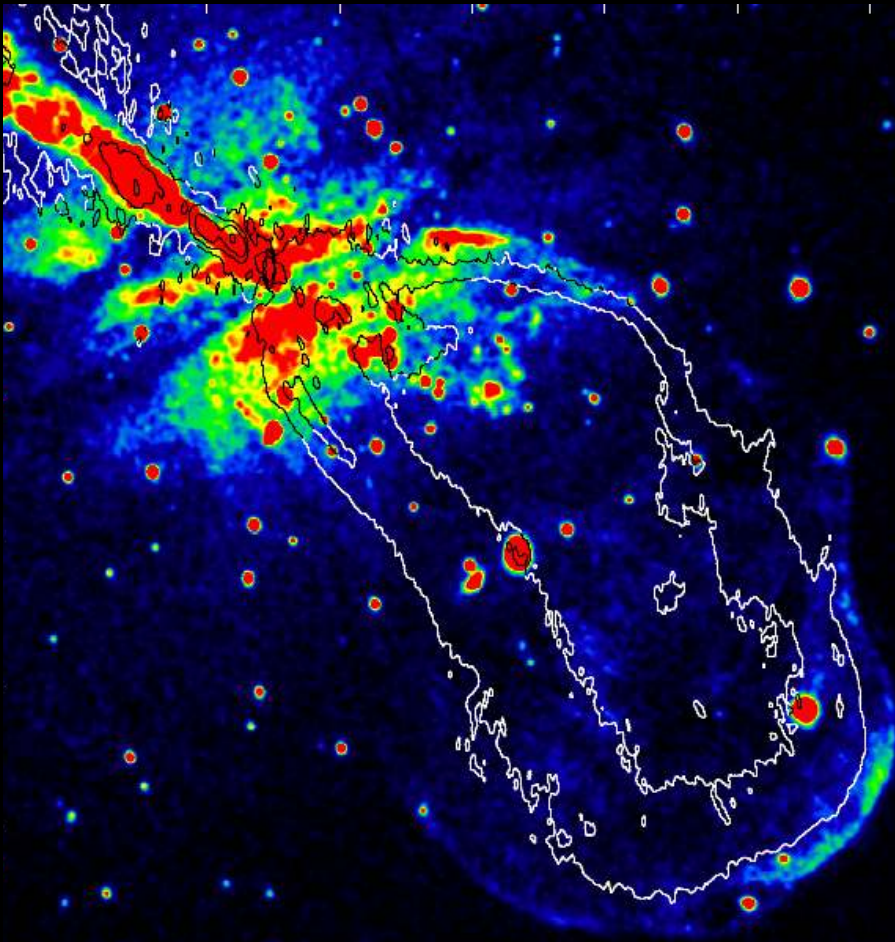
Dan Evans

Preeti Kharb

Ananda Hota

the Cen A ChandraVLP collaboration

# Magnetic field strength constraints



- The shock front appears resolved in the Chandra data, so its width can be used to determine  $B$ , assuming synchrotron losses dominate
- Using method of Vink & Laming (2003), we find synchrotron lifetimes of  $\sim 5 \times 10^4$  y  $\Rightarrow B \sim 1 \mu\text{G}$ .
- Consistent with equipartition calculations ( $B < 8.5 \mu\text{G}$  for  $\kappa=1$ ) & consistent with expectation from compression of the ISM if  $B_{\text{ISM}} \sim 0.1 - 1 \mu\text{G}$ .

# Electron-proton equilibration

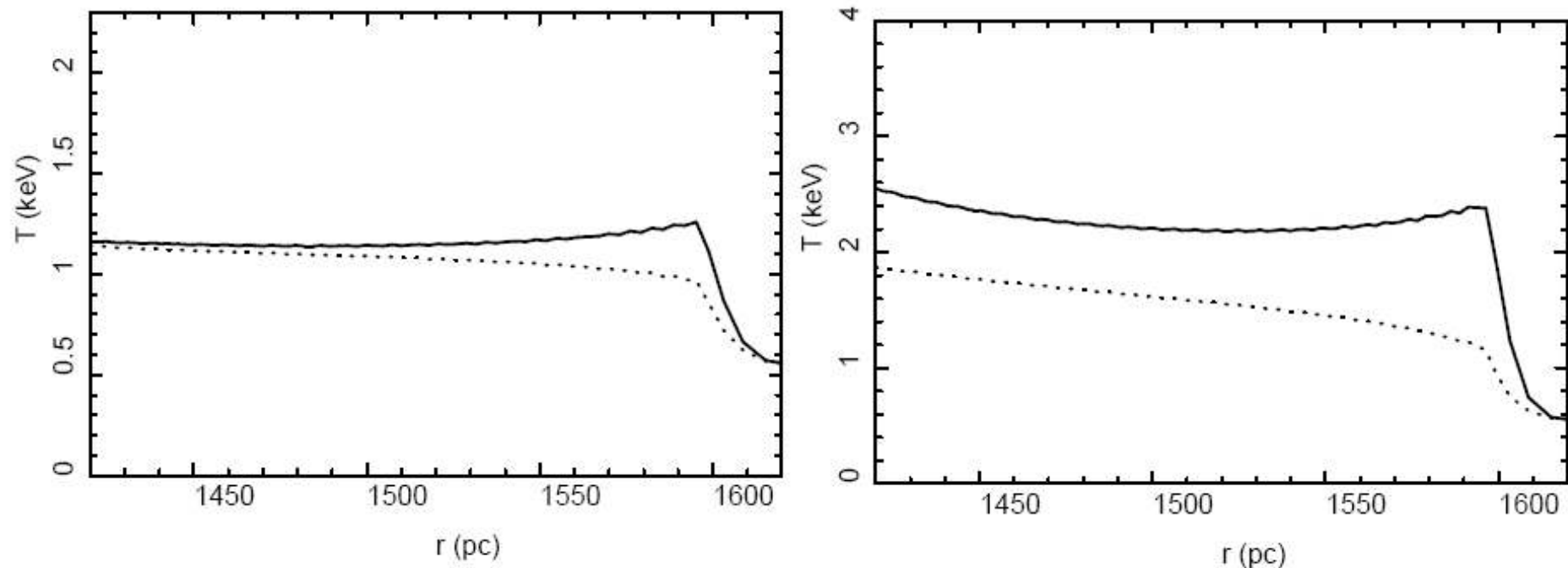
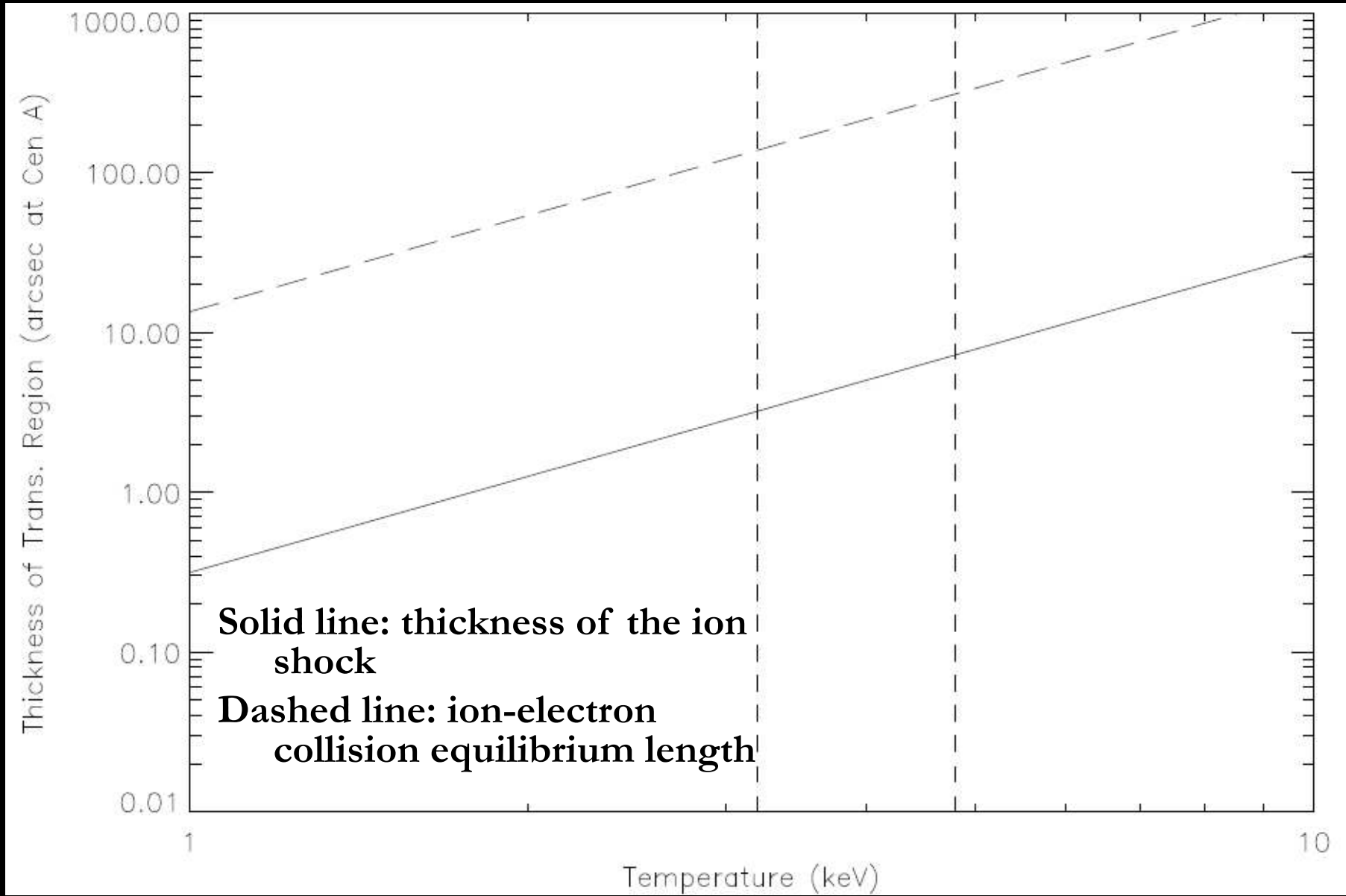


Fig. 7.— Post-shock proton temperature (solid line) and electron temperature (dotted line) profiles obtained from our two-fluid hydrodynamical modelling (§ 4.4) for  $kT = 1$  keV (left) and  $kT = 1.4$  keV (right).



**Kraft et al. 2007**

# Spectra for the shell region

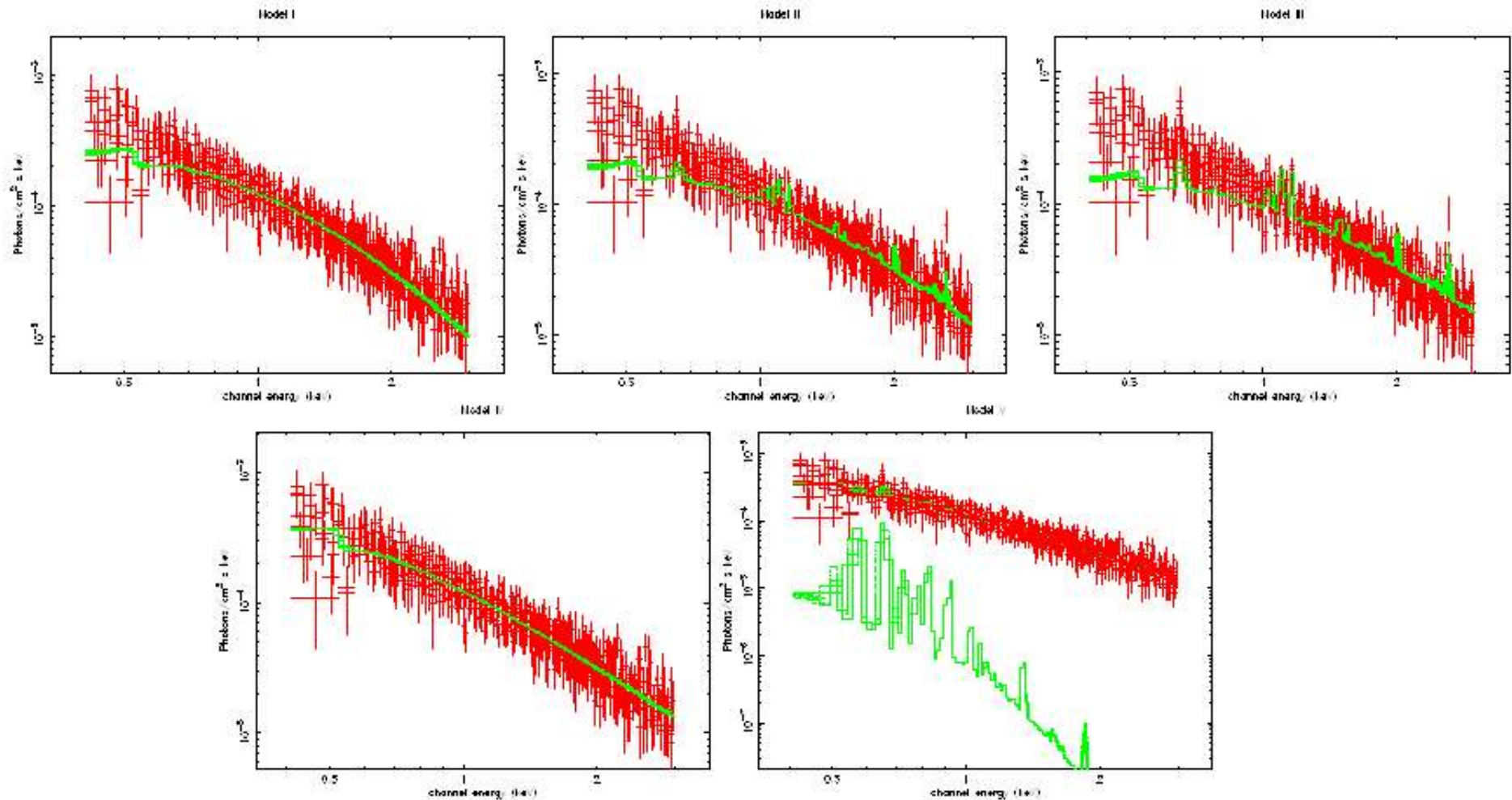


Fig. 4.— Spectral fits for Region 1. Clockwise from top left: Model I (free-abundance *apec*), Model II (*apec* with  $Z = 0.15Z_{\odot}$ ), Model III (*apec* with  $Z = 0.5Z_{\odot}$ ), Model V (power law + *apec*), and Model IV (power law).

# Shell spectra (2)

| Model      |                               | Parameter         | Region 1               | Region 2               | Region 3               |
|------------|-------------------------------|-------------------|------------------------|------------------------|------------------------|
| Model I:   | <i>apec</i> (free abundance)  | $kT$ (keV)        | $1.60^{+0.07}_{-0.06}$ | $2.03^{+0.24}_{-0.14}$ | $0.91^{+0.04}_{-0.04}$ |
|            |                               | $Z (Z_{\odot})$   | $< 0.007$              | $< 0.05$               | $0.17^{+0.05}_{-0.04}$ |
|            |                               | $\chi^2$ (d.o.f.) | 1010 (743)             | 344 (308)              | 137 (97)               |
| Model II:  | <i>apec</i> (fixed abundance) | $kT$ (keV)        | $2.22^{+0.08}_{-0.06}$ | $2.59^{+0.13}_{-0.13}$ | $0.90^{+0.03}_{-0.02}$ |
|            |                               | $Z (Z_{\odot})$   | 0.15                   | 0.15                   | 0.15                   |
|            |                               | $\chi^2$ (d.o.f.) | 1213 (744)             | 377 (309)              | 138 (98)               |
| Model III: | <i>apec</i> (fixed abundance) | $kT$ (keV)        | $3.26^{+0.09}_{-0.09}$ | $3.58^{+0.24}_{-0.19}$ | $0.97^{+0.01}_{-0.02}$ |
|            |                               | $Z (Z_{\odot})$   | 0.5                    | 0.5                    | 0.5                    |
|            |                               | $\chi^2$ (d.o.f.) | 1478 (744)             | 437 (309)              | 177 (98)               |
| Model IV:  | <i>power law</i>              | $\Gamma$          | $2.20^{+0.02}_{-0.02}$ | $2.01^{+0.04}_{-0.03}$ | $2.54^{+0.05}_{-0.05}$ |
|            |                               | $\chi^2$ (d.o.f.) | 931 (744)              | 333 (309)              | 445 (98)               |
| Model V:   | <i>apec + power law</i>       | $kT$ (keV)        | $0.23^{+0.09}_{-0.08}$ | $0.93^a$               | $0.89^{+0.05}_{-0.06}$ |
|            |                               | $Z (Z_{\odot})$   | 0.5                    | 0.5                    | 0.5                    |
|            |                               | $\Gamma$          | $2.15^{+0.06}_{-0.05}$ | $2.00^{+0.15}_{-0.06}$ | $2.13^{+0.30}_{-0.27}$ |
|            |                               | $\chi^2$ (d.o.f.) | 928 (742)              | 332 (307)              | 141 (96)               |